Vol. 22, No. 3(2023) Ener3030
Revista Mexicana de Ingeniería Química

A comparative study of different poly(3-hexylthiophene)-carbon based hole transport layers on the stability of perovskite solar cells prepared under ambient conditions

Un estudio comparativo de diferentes compuestos de poli(3-hexiltiofeno)-carbono como capas transportadoras de huecos sobre la estabilidad de celdas solares de perovskita preparadas bajo condiciones ambientales

C.F. Arias-Ramos[1,§], F. Hernández-Guzmán[1,§], J. Camacho-Cáceres[1,§], D. K. Becerra-Paniagua[1], W. R. Gallegos-Pérez[1], M. A. Millán-Franco[1], M. E. Nicho[2], H. Hu[1*]

[1]*Instituto de Energías Renovables, Universidad Nacional Autónoma de México (UNAM), Privada Xochicalco S/N, Temixco, Morelos, 62580, México.*

[2]*Centro de Investigación en Ingeniería y Ciencias Aplicadas, Universidad Autónoma del Estado de Morelos, Av. Universidad 1001, Cuernavaca, Morelos, 62209, México.*

Received: December 6, 2022; Accepted: March 9, 2023

Abstract

Hole transport layers (HTLs) play an important role in efficiency and stability of perovskite solar cells (PSCs). Most of the highly efficient PSCs use spiro-OMeTAD doped with Li-TFSI as HTLs, which has to be prepared under inert atmosphere, because the hygroscopic feature of the lithium salt deteriorates the stability of PSCs under ambient conditions. In this work, we report a comparative study of the electrical and morphological properties of different poly(3-hexylthiophene) (P3HT) thin films: pristine, doped with $FeCl_3$, and composites with carbon nanotubes (CNT) or reduced graphene oxide (rGO). Although the electrical conductivity of P3HT films is found to increase with any of those modification methods, the photovoltaic performance of PSCs is highly dependent on the modification agent. P3HT:$FeCl_3$ reduces the photocurrent density of PSCs, while the addition of rGO in P3HT improves charge extraction and stability of PSCs. Furthermore, the insertion of conductive carbon paint between P3HT and the metal contact maintains the original efficiency of non-encapsulated PSCs after continuous illumination for 30 min. It is concluded that carbon modifications in P3HT based HTL can improve the stability of perovskite solar cells totally fabricated under ambient conditions.

Keywords:perovskite solar cells, poly(3-hexylthiophene), reduced graphene oxide, carbon nanotube, composite polymer thin films.

Resumen

Las capas de transporte de huecos (HTL) juegan un papel importante en la eficiencia y la estabilidad de las celdas solares de perovskita (PSCs). Las más eficientes PSCs usan spiro-OMeTAD como HTL que contiene una sal de litio, lo cual deteriora la estabilidad de las PSCs en condiciones ambientales. En este trabajo, reportamos un estudio comparativo de las propiedades eléctricas y morfológicas de películas delgadas de poli(3-hexiltiofeno) (P3HT) dopado con $FeCl_3$, o bien, compuestas con nanotubos de carbono (CNT) u óxido de grafeno reducido (rGO). Se encuentra que la conductividad eléctrica de las películas de P3HT aumenta con cualquiera de esos métodos de modificación, y el rendimiento fotovoltaico de las PSCs depende del agente de modificación. P3HT:$FeCl_3$ induce una reducción notable en la densidad de fotocorriente de las PSCs, mientras que la P3HT:rGO mejora la extracción de carga y la estabilidad de las PSCs. Además, la inserción de pintura conductora de carbono entre P3HT y el contacto de oro mantiene la eficiencia original de las PSC sin encapsulación después de una iluminación continua durante 30 min. Se concluye que los compuestos de P3HT con materiales de carbono pueden mejorar la estabilidad y eficiencia de las celdas solares de perovskita.

Palabras clave: celdas solares de perovskita, poli(3-hexiltiofeno), óxido de grafeno reducido, nanotubos de carbono, películas delgadas poliméricas compuestas.

* *Corresponding author. E-mail*: hzh@ier.unam.mx
§The three authors contribute equally to this work.
https://doi.org/10.24275/rmiq/Ener3030
ISSN:1665-2738, *issn-e*: 2395-8472

1 Introduction

Perovskite solar cells (PSCs) are the most efficient emerging solar cells prepared from chemical solutions, providing more than 25% power conversion efficiency (*PCE*) in a small area (Green *et al*., 2019). The basic structure of PSCs consists of an electron transport layer (ETL), an absorbing hybrid perovskite thin film, a hole transport layer (HTL) and a metal contact. In most efficient PSCs, the perovskite and HTL layers are fabricated under inert atmosphere and the non-encapsulated PSCS are even tested in nitrogen filled ambient to avoid contact with humidity (Joshi *et al*., 2016). The use of inert gas (N_2) for the manufacture of perovskite solar cells is not cost effective, which make them far from the commercialization. Several review works discuss the challenges of air-processed PSCs, from the mechanism of degradation of perovskite thin films in contact with moisture to the standardization of stability tests (Krishna *et al*., 2021; Younas *et al*., 2021; Sharma *et al*., 2022). Among all steps of the PSC production, the selection of the HTL layer also plays an important role in the stability of PSCs.

Spiro-OMeTAD is a molecular semiconductor material that has been used as HTLs in most efficient PSCs. The highest occupied molecular orbital (HOMO) and lowest unoccupied molecular orbital (LUMO) of spiro-OMeTAD, ~5.0 (Snaith *et al*., 2007; Ono *et al*., 2014) and ~1.7 eV (Ono *et al*., 2014), respectively, make it an effective hole transporter and electron blocker for the perovskite layer with a HOMO level of ~5.4 eV and LUMO level of ~3.8 eV (Schulz *et al*., 2014). Most of the spiro-OMeTAD based HTLs contain a lithium salt (Li-TFSI), which improves its electric conductivity, but at the same time, makes it very hygroscopic to require an inert ambient for its preparation. The addition of reduced graphene oxide (rGO) to both halide perovskite and spiro-OMeTAD is reported to increase the efficiency and stability of PSCs (Kim *et al*., 2020).

Another organic semiconductor, poly(3-hexylthiophene) (P3HT), has also been used as HTLs in PSCs. P3HT has almost the same HOMO level as spiro-OMeTAD, 5.0-5.1 eV. However, its LUMO level is higher (~ 3.0 eV) than that of spiro-OMeTAD (~ 1.7 eV), leading to a larger charge carrier recombination at the perovskite/P3HT interface and consequently making it less effective as an electron blocker. To reduce such recombination, several interfacial modification strategies have been reported (Jung *et al*., 2019; Zhang *et al*., 2020; Jeong *et al*., 2021; Peng *et al*., 2022; Guo *et al*., 2021; Gu *et al*., 2022; Kassem *et al*., 2022; Ghoreishi *et al*., 2022; Li *et al*., 2022). The most successful one has been the introduction of a thin layer of wide-bandgap halide perovskite on the perovskite surface (Jung *et al*., 2019), together with the addition of gallium (III) acetylacetonate in P3HT, leading to very efficient (~ 24%) and stable PSCs (Jeong *et al*., 2021). Strategies of adding carbon nanotubes (CNT) (Habisreutinger *et al*., 2014) or rGO into P3HT (Chu *et al*., 2019) have also been used to improve the efficiency of P3HT-based PSCs from 11% to 18% (Chu *et al*., 2019). On the other hand, P3HT of very high molecular weight (100-300 kDa) and doped with Li-TFSI, TBP and FK209-Co(III)-TFSI, has been used as HTL in air-prepared PSCs, reaching efficiency of 19.25% in a small area with a multication perovskite ($(FAPbI_3)_{0.81}(MAPbBr_3)_{0.14}(CsI)_{0.05}$) (Nia *et al*., 2017; Nia *et al*., 2018; Nia *et al*., 2019; Nia *et al*., 2021). In those cases, the non-encapsulated PSCs lost about 20% of their efficiencies after 1500 h (62.5 days) of storage in air, and the continuous illumination test was performed only for the encapsulated PSCs (Nia *et al*., 2019). Dopant-free P3HT has also been reported as HTL in PSCs, prepared under ambient conditions, with a maximum efficiency of 16.23% when using formamidine iodide (FAI) as an intermediate phase at the surface of $MAPbI_{3-x}Cl_x$ (Wu *et al*., 2021). This interfacial treatment raises the edge of the valence band of the perovskite, leading to better match with the HOMO of P3HT, and consequently faster charge extraction at the anode of the PSCs. However, in this case there is no information about the cell stability over a relatively long storage period.

We have prepared perovskite thin films under ambient conditions (60% relative humidity at 22 to 26°C) by adding a hydrophobic additive in anti-solvent to increase the moisture resistivity of perovskite thin films, and the best PSCs achieved efficiencies close to 17% with spiro-OMeTAD layers deposited in a nitrogen environment (Arias-Ramos *et al*., 2020). These non-encapsulated PSCs maintained 80% of the original efficiencies after 6 months of storage at ambient conditions. But a much more realistic stability test is under continuous light illumination for non-encapsulated PSCs. We found that after only continuous illumination for 27 min, those cells retained 80% of their original efficiencies (Torres-Herrera *et al*., 2020), that is, the same values retained when stored in air for 6 months.

Based on previous reports, we propose a comparative study on the photovoltaic behavior of

PSCs by using doped or composite P3HT as HTL, which should be electrically more conductive than the pristine (or dopant free) P3HT, and, at the same time, provide a good stability to PSCs. In this work, pristine P3HT with a molecular weight of about 28 kDa was synthesized and doped with $FeCl_3$. The P3HT-rGO and P3HT-Carbon nanotubes (CNT) composites have also been prepared with different weight percentage (wt%) of rGO and CNT in P3HT. The simplest perovskite compound, $MAPbI_{3-x}Cl_x$, has been chosen for solar cell fabrication without any interfacial modification. The entire PSC manufacturing process has been carried out in an ambient atmosphere with a relative humidity of 35-60% at 22-26°C. Although high relative humidity and oxygen concentration can oxidize P3HT (Arenas *et al*., 2010), we believe that the oxidation process of P3HT should be slower than the hydration of hygroscopic dopants (Li-TFSI) in HTL. The results of this work confirm that P3HT-rGO composite films not only show a higher electrical conductivity, but also provide a better protection for the perovskite layers against moisture and ambient oxygen. Furthermore, with the addition of conductive carbon paint on top of P3HT, non-encapsulated PSCs with P3HT as HTLs maintain their original efficiency after continuous illumination for 30 min, the best stability reported in similar PSCs.

2 Materials and methods

All device sample preparation and characterization in this work were carried out under ambient condition at 23-27 °C and 35-65% relative humidity, unless otherwise stated. The temperature and relative humidity (RH) of our laboratory were recorded with a hygrometer (UNI-T, UT333BT) with a temperature accuracy of ±1 °C, and a humidity accuracy of ±5%.

2.1 Deposition of different P3HT thin films

The regioregular P3HT was synthesized by Grignard metathesis polymerization (Loewe *et al*., 1999; Hernández-Guzmán *et al*., 2017) with an average molecular weight (MW) of about 28 kDA (Hernández-Guzmán *et al*., 2017). Graphene oxide (GO) products were synthesized using a modified Tour method (Becerra-Paniagua *et al*., 2019). Reduced graphene oxide (rGO) products were produced by chemical reduction of GO (Becerra-Paniagua *et al*., 2020). Commercial products of single-walled carbon nanotubes (CNT, Sigma-Aldrich) were used as purchased.

Four types of P3HT solutions were prepared: (1) pristine P3HT in chlorobenzene (CB, 99.5%, Sigma-Aldrich) or 1,2,4-Trichlorobenzene (TCB, 99% anhydrous Sigma-Aldrich) with concentrations of 10 to 25 mg/mL; (2) a 20 mg/mL P3HT solution in CB doped with 1, 2 or 8 mM of $FeCl_3$ (previously dissolved in CB or TCB) called as P3HT-1mM, P3HT-2mM or P3HT-8mM; (3) mixture solutions of P3HT-rGO in CB with different percentages by weight of rGO: 10, 20, 30, 40 and 50 wt%; (4) mixture solutions of P3HT-CNT in CB with different percentages by weight of CNT: 1, 3, 5, 10 and 15 wt%. Several drops of 1,8-diiodooctane were added to the P3HT-rGO or P3HT-CNT mixtures to improve the dispersion of rGO or CNT in the P3HT solution. P3HT thin films were deposited on glass or perovskite substrates by spin-coating at 2500 rpm for a drying time of 40 to 150 s, depending on the type of solvent, and followed by thermal annealing at 100 °C for 5 min. Table 1 contains the information of the P3HT samples studied in this work.

Table 1. Samples of pristine, doped and composite P3HT thin films.

P3HT thin films	Sample name	Thickness (nm)
P3HT pristine	P3HT	30-50
P3HT doped with 1, 2 or 8 mM $FeCl_3$	P3HT-X mM, where X = 1, 2 or 8.	50-80
P3HT composite with carbon nanotube (CNT) of 1, 3, 5, 10, 15 or 35 wt%	P3HT-CNTX, where X = 1, 3, 5, 10, 15 or 35.	40-60
P3HT composite with reduced graphene oxide (rGO) of 10, 20, 30, 40 or 50 wt%	P3HT-CNTX, where X = 10, 20, 30, 40 or 50.	35-70

2.2 *Fabrication of perovskite solar cells*

Perovskite solar cells were fabricated in ambient atmosphere with a similar procedure reported previously (Arias-Ramos *et al.*, 2020). Briefly, fluorine-doped tin oxide (FTO) substrates (TEC 15 glass, Great Cell Solar) were patterned by chemical etching with zinc powder and HCl (3 M). After then they were washed with detergent, distilled water and acetone, followed by sonication for 10 min in isopropanol and cleaning under UV ozone for 15 min. To prepare compact titanium oxide (c-TiO_2) thin films, a titanium precursor solution was prepared by mixing 20 mL isopropanol, 1.2 mL titanium isopropoxide (97%, Aldrich), and 0.4 mL hydrochloric acid. The resulting solution was sonicated for 30 min and deposited onto clean and patterned FTO glass substrates by spin-coating for 30 s at 3000 rpm. The precursor coating samples were then heated in an air oven at 450 °C for 30 min. The average thickness of c-TiO_2 is about 40 nm. TiO_2 paste (30NRD, Great Solar Cell) was diluted in ethanol in a 1:6 wt ratio and then spin-coated on a c-TiO_2 at 4000 rpm for 30 s. After thermal annealing in air at 500 °C for 30 min, a mesoporous layer of TiO_2 (m-TiO_2) was formed on c-TIO_2. The average thickness of m-TiO_2 was approximately 220 nm.

A hybrid halide perovskite ($CH_3NH_3PbI_{3-x}Cl_x$) precursor solutions was prepared by mixing lead iodide (PbI_2, 99.999%, Lumtec), methylammonium iodide (MAI, 99.5%, Lumtec), methylammonium chloride (MACl, 99.5%, Lumtec) and dimethyl sulfoxide (DMSO, 99.9%, Sigma-Aldrich) in a PbI_2:MAI:MACl:DMSO = 1:1:0.05:1 M molar ratio in 1 mL of dimethylformamide (DMF, 99.8%, Sigma-Aldrich). The perovskite solution was stirred at 500 rpm for 24 h under ambient conditions. The deposition of the perovskite solution started after its complete coverage on the m-TiO_2 layer with a spin speed of 5000 rpm for 20s. After several seconds, an anti-solvent was added to the coating, consisting of 140 μL of ethyl acetate (EA, 99.8% anhydrous, Sigma-Aldrich) and a small amount of ionic surfactants such as 4-tert-butylpyridine. The obtained MAPbI3-xClx coatings were heated at 100 °C for 2 min and converted into solid perovskite thin films. The average thickness of the perovskite coating on m-TiO_2 is about 350 nm.

As HTLs, P3HT solutions were spin-coated on perovskite surface at 2500 rpm for 40 s, followed by a thermal annealing at 100 °C for 5 min in air. For comparative purposes, spiro-OMeTAD-based

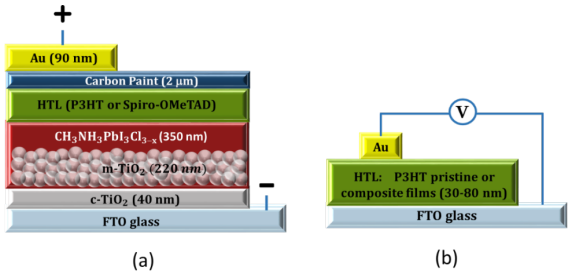

Scheme 1. Cross-section of (a) a perovskite solar cell and (b) a hole-only device (not in scale).

HTL with a composition described in the reference (Arias-Ramos *et al.*, 2020) was also deposited on perovskite under ambient conditions. An optional layer of carbon paint (CP) was sprayed over the P3HT (Cortina-Marrero *et al.*, 2013). Finally, the gold (Au) contact was thermally evaporated over the P3HT layers in a high vacuum chamber of 2.6×10^{-5} Torr. The cross-sectional geometric structure of our PSCs can be seen in Scheme 1a.

2.3 *Material and device characterization*

Optical absorbance spectra of P3HT films were measured in a spectrophotometer (Shimadzu UV-1800) in the wavelength range of 200 to 1100 nm. The electrical current-voltage (I-V) curves of P3HT films were measured in the dark in hole-only devices: FTO/P3HT/Au (Scheme 1b), and the cross-sectional area of all these hole-only devices was of 0.3 cm^2. A digital Keithley 2400 four-wire source unit was used to measure the current versus voltage (I-V) curves. The thickness of P3HT films was measured with an AMBIOS Technology XP-200 profilometer, which ranged from approximately 30 to 80 nm. Atomic force microscopy (AFM) analysis was performed on a Veeco Dimension Icon equipment with Scan Asyst at different scales.

The photovoltaic performance of PSCs was evaluated by measuring their I-V curves under illumination in an Oriel 81,174 class AAA equipped solar simulator under AM 1.5G with a Keithley 2400 source meter as data acquirer under ambient conditions, with the voltage scan direction from 1.1 to -0.1 V. The light intensity was 100 mW/cm^2, calibrated with a Newport Si reference cell. The active test area of all PSCs was of 0.104 cm^2, which was delimited through a metallic mask. The PSC samples used for the stability study were stored in the dark under environmental conditions and their I-V curves were measured under continuous illumination

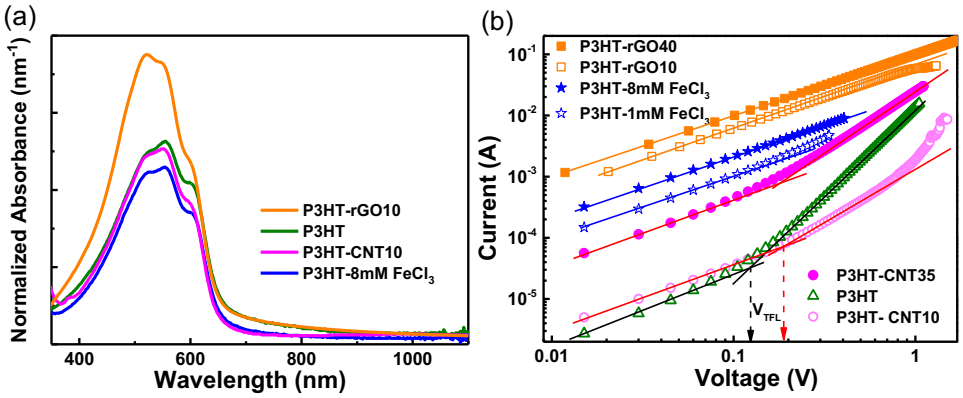

Figure 1. (a) Normalized optical absorbance spectra with respect to film thickness and (b) Dark current-voltage curves of P3HT, $FeCl_3$ doped-P3HT, P3HT-rGO and P3HT-CNT thin films.

at ambient conditions. All the PSCs prepared and studied in this work were non-encapsulated.

3 Results and discussion

The pristine or intrinsic P3HT is modified by $FeCl_3$ doping or the addition of different forms of carbon compounds (CNT and rGO). Fig.1a shows normalized optical absorbance spectra with respect to film thickness of three types of P3HT thin films. It is observed that when the P3HT solution was doped with $FeCl_3$ of different concentration, from 1 mM to 8 mM, the corresponding P3HT films (P3HT-8mM, blue curve) keep the same absorption spectra as the pristine P3HT (green curve) with a slightly lower absorption intensity. In this case broad bipolaronic bands do not appear around 800 nm, as occurred when P3HT is oxidized, leading to the suggestion that at a relatively low concentration $FeCl_3$ molecules do not oxidize the main chains of P3HT. On the other hand, the P3HT- CNT 10 wt% composite thin film also provides a similar optical absorbance spectrum (pink curve, Fig.1a), and the P3HT-rGO 10wt% sample shows the highest optical absorbance spectrum per unit of thickness (orange curve) compared to other P3HT films.

Fig. 1b shows the transverse electrical current (I) vs. applied voltage (V) curves of pristine, doped and composite P3HT thin films in the hole-only device configuration (Scheme 1b). The pristine P3HT film (hollow green triangles) shows a voltage-dependence transition at a critical voltage value, called as tramp filled limit voltage (V_{TFL}), equal to about 0.12 V. For a voltage less than 0.12 V, the current of pristine P3HT hole-only device gives a linear or ohmic behavior, $I = V/R$ (R = resistance of the film sample in the direction of the film thickness). For $V > 0.12$ V, it exhibits a nonlinear, Space Charge Limited Current (SCLC) behavior described by the Mott-Gurney relation for intrinsic semiconductor thin films: $I = A\frac{9}{8}\varepsilon_0\varepsilon_r\mu\frac{V^2}{d^3}$, where A is the cross-sectional area of the film, ε_0 the vacuum permittivity, ε_r the relative permittivity, μ the charge carrier mobility and d the film thickness. As expected, the electrical feature of pristine P3HT thin films is characteristic of a trap-free dielectric or intrinsic semiconductor material (Kwan *et al.*, 2019).

When P3HT is doped with $FeCl_3$, the $I-V$ curves of the films become mostly ohmic. Fig.1b shows that for P3HT doped with 1 mM $FeCl_3$ (hollow blue stars), the I-V curve is linear at voltages lower than 0.2 V; after that, the curve shows a very small deviation from the straight line. For P3HT doped with 8 mM $FeCl_3$ (solid blue stars), the I-V curve becomes a straight line, completely losing the SCLC characteristics of intrinsic semiconductor materials. The same ohmic behavior is also observed in the P3HT-rGO composite films (hollow and solid orange squares in Fig.1b). Both 10 and 40 wt% of rGO in P3HT matrices produce a linear relationship between electrical current and applied potential. Furthermore, considering the small difference in film thickness among all P3HT films, Fig.1b suggests that P3HT-rGO films are more conductive than $FeCl_3$-doped P3HT films. Finally, P3HT-CNT composites behave differently than P3HT-rGO. Fig.1b shows how P3HT-CNT 10 and 35 wt% thin films give non-linear I-V curves (hollow and solid pink circles) like intrinsic semiconductors, with a higher V_{TFL} value (close to

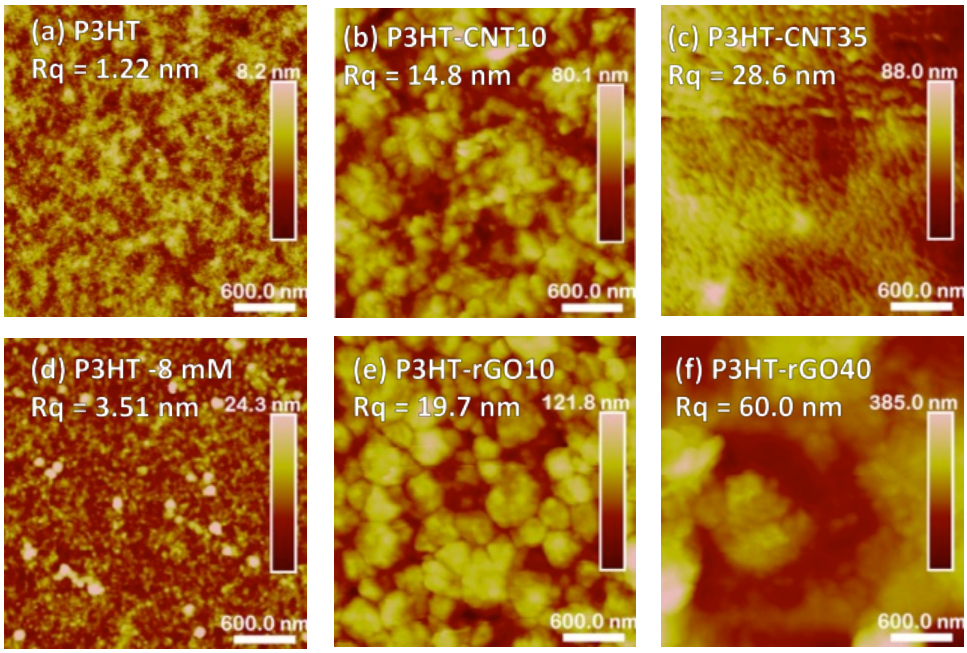

Figure 2. AFM images in 3 μm^2 and root mean square roughness values in 10 μm^2 (R_q) of (a) P3HT, (b) P3HT-CNT 10wt%, (c) P3HT-CNT 35wt%, (d) P3HT doped with 8 mM $FeCl_3$, (e) P3HT-rGO 10wt%, and (f) P3HT-rGO 40wt% thin films.

0.2 V). Higher concentration of CNT in P3HT results in higher conductivity without losing the SCLC characteristic of P3HT-CNT composite films.

The different electrical properties of P3HT composite films may come from different geometric structures of rGO and CNT: two-dimensional graphene (rGO) versus one-dimensional carbon nanotubes (CNT). Fig.2 shows AFM images of 3 μm^2, as well as the root mean square roughness values of 10 μm^2 (R_q), of six P3HT thin film samples. Pristine P3HT has a very smooth surface with R_q equal to 1.16 nm (Fig.2a). The addition of CNT increases the surface roughness up to 14.8 nm when the concentration of CNT in P3HT is 10 wt% (Fig.2b) and up to 28.6 nm if such concentration is 35 wt% (Fig.2c). $FeCl_3$ doping in P3HT only slightly increases the roughness of P3HT (3.53 nm, Fig.2d). However, the addition of rGO in P3HT induces higher roughness in P3HT-rGO composite films; with 10 wt% rGO, the P3HT-rGO10 film shows an R_q value of 19.7 nm (Fig.2e) and with 40 wt% of rGO, this value is up to 60.0 nm (Fig.2f). The difference in surface roughness of the two types of P3HT composite films suggests that the orientation of the carbon nanotubes might be along the film surface, while the graphene sheets might be randomly distributed within the P3HT matrix.

To achieve a good power conversion efficiency (PCE), the energy levels of all layers in a PSC should be properly arranged to facilitate charge generation and transport. Fig.3a illustrates the energy levels of the electron transport (TiO_2), perovskite, and hole transport (spiro-OMeTAD or P3HT) layers in a PSC. Fig.3b shows the J-V curves under illumination of PSCs with 3 different HTLs, all prepared under ambient conditions: spiro-OMeTAD (olive green), pristine P3HT (red), and P3HT doped with 8 mM $FeCl_3$ (blue). All three types of PSCs have similar values of open circuit voltage (V_{OC}). As expected, the spiro-OMeTAD-based PSC provides the highest short-circuit current density (J_{SC}), consequence of a lower LUMO level or lower charge recombination rate at the perovskite/spiro-OMeTAD interface. However, this particular spiro-OMeTAD-based solar cell shows an "S"-like J-V curve, that is, a very low fill factor (FF) ~ 0.40, defined as: $FF = (J_{\max}V_{\max})/(J_{SC}V_{OC})$, with $J_{\max}V_{\max} = P_{\max}$ as the maximum power that the solar cell can produce. $J - V$ curves with "S" shape are observed in some of low efficient perovskite solar cells, specifically those with degraded perovskite layers. The degradation of perovskite could originate from its inadequate preparation process, or from the adjacent ETL or HTL of poor quality.

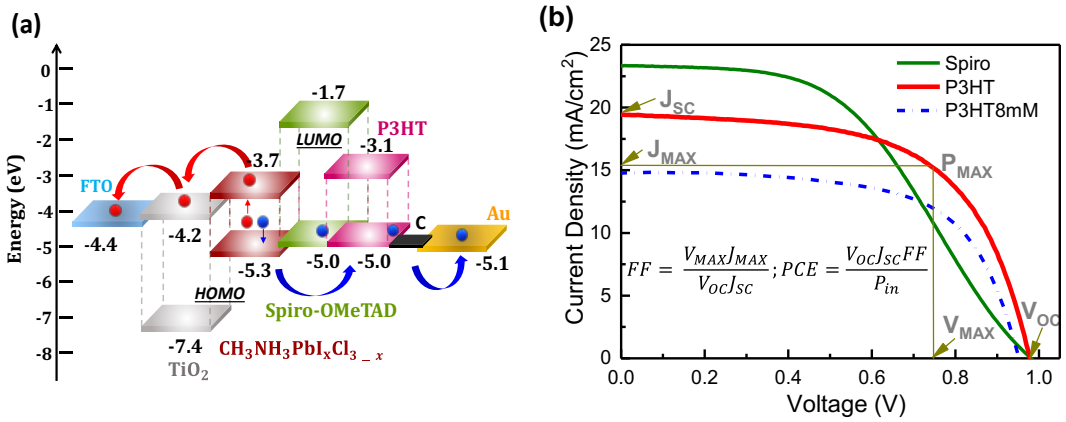

Figure 3. (a) Energy levels in perovskite solar cells with spiro-OMeTAD or P3HT as HTL. “C" means conductive carbon paint. (b) Current density vs. voltage of perovskite solar cells under 1 Sun illumination with spiro-OMeTAD, pristine P3HT, or $FeCl_3$ doped (8 mM) P3HT as HTL, all prepared under ambient conditions.

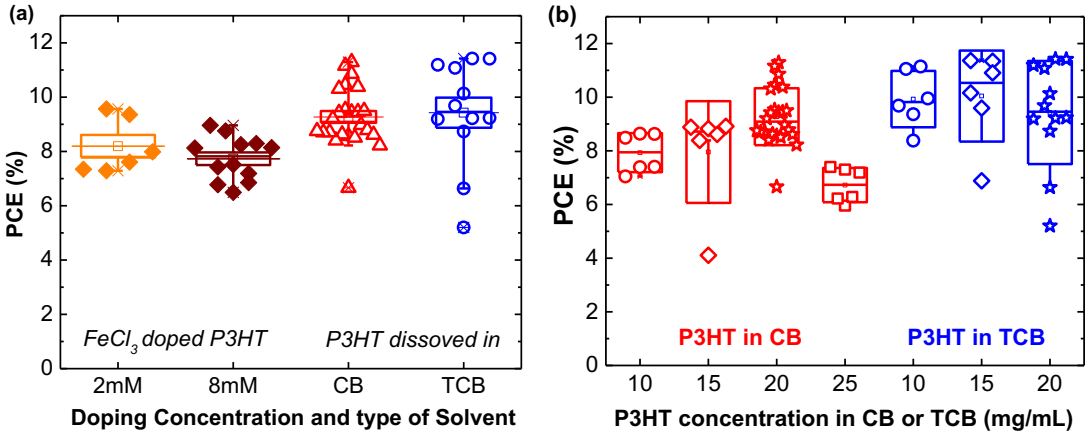

Figure 4. PCE of P3HT-based PSCs in which P3HT layers were prepared with: (a) $FeCl_3$ doped (2 o 8 mM) P3HT and pristine P3HT in different solvents (CB and TCB), in which P3HT concentration was 20 mg/mL; (b) pristine P3HT of different concentration in CB and TCB solutions.

In this case, spiro-OMeTAD layer was prepared under ambient atmosphere and was highly hygroscopic. As a result, the water molecules should be present as impurities at the perovskite/spiro-OMeTAD interface. When the perovskite layer is in contact with water molecules, the acid-base Lewis reaction occurs (Frost *et al.*, 2014; Kim *et al.*, 2016), leading to the decomposition of MAPbI3 (dark, semiconductor) into MAI+ PbI_2 (yellow, insulate). The MAI+PbI_2 insulate layer should be the origin of the “S" shape J-V curve observed in Fig.3b. The same PSCs but with spiro-OMeTAD layers prepared in a nitrogenous environment reported higher FF values (~0.70) (Arias-Ramos *et al.*, 2020). On the other hand, P3HT-based PSCs, prepared under the same ambient conditions, give higher FF values (0.60-0.65) compared to spiro-OMeTAD, as indicated in Fig.3b. This confirms our hypothesis that P3HT is more stable than spiro-OMeTAD doped with lithium salt when both are prepared under ambient conditions. Finally, PCE of a solar cell is defined as: $PCE = P_{\max}/P_{in}$, where P_{in} is the intensity of the incident light (Fig.3b).

At the same time, Fig.3b also suggests that $FeCl_3$ doped P3HT significantly reduces the J_{SC} value and consequently the PCE values of the corresponding PSCs. Furthermore, Fig.4a indicates that pristine P3HT-based PSCs have on average 1 or 2 % higher PCE values than those PSCs with 2 mM or 8 mM $FeCl_3$-doped P3HT as HTLs, and the higher the $FeCl_3$ doping concentration, the lower the PCE values. Since

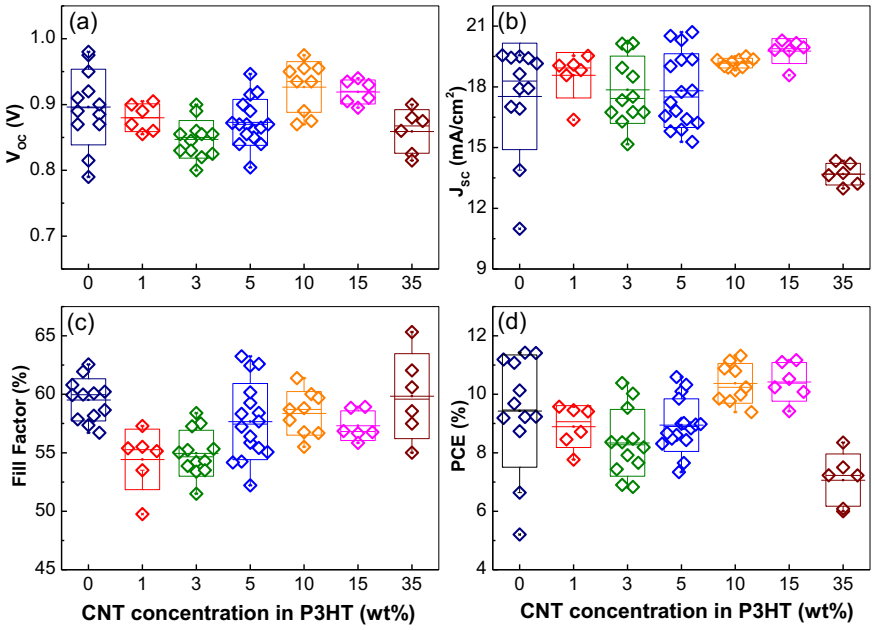

Figure 5. (a) V_{OC}, (b) J_{SC}, (c) FF and (d) PCE of PSCs with P3HT-CNT composite films as hole transport layers. The weight percentage of CNT in P3HT varies from 1 to 35wt%.

$FeCl_3$-doped P3HT thin films do not contain bipolaronic bands within the P3HT bandgap (Fig.1a), we can infer that $FeCl_3$ molecules introduce impurity energy levels in the P3HT bulk material, which increase the charge carrier combination rate at perovskite/P3HT interface and reduce the J_{SC} and PCE values of the corresponding PSCs.

In addition, Fig.4 exhibits the effect of the type of solvent as well as concentration of P3HT solutions on the efficiency of PSCs. Statistically, pristine P3HT-based PSCs show similar PCE values when either chlorobenzene (CB, solid red squares, Fig.4a) or 1,2,4-trichlorobenzene (TCB, solid blue squares, Fig.4a) was used as P3HT solvent, for the same P3HT concentration (20 mg/mL). However, if such concentration is changed, the result may also differ, as indicated in Fig.4b. When a lower boiling solvent CB (98 °C) is used, the drying time of P3HT-CB coatings is shorter (less than 40 s). With such a fast drying process, very low (10 mg/mL) or high (25 mg/mL) concentrations of P3HT solutions can leave non-uniform P3HT films on perovskite surface, resulting in a non-homogeneous contact with the up-coming metal contact, and consequently less efficient PSCs result in (Fig.4b). On the other hand, for a higher boiling solvent like TCB (213 °C), the drying time of P3HT-TCB coatings is much longer during spin-coating (1.5-2 min). As a result, the P3HT molecules have enough time to distribute uniformly on the perovskite surface, regardless of P3HT concentration in TCB, giving homogeneous P3HT coatings and similar *PCE* statistics of the corresponding PSCs (Fig.4b).

On the other hand, due to the similar electrical properties of P3HT-CNT composite films compared to the pristine P3HT, the addition of CNT in P3HT shows negligible influence on the photovoltaic performance of P3HT-based PSCs. Fig.5 indicates that for CNT percentages from 1 to 35 wt%, the V_{OC} (Fig.5a) and FF (Fig.5c) values fluctuate slightly without a clear pattern with CNT concentration. Only J_{SC} values (Fig.5b) remain statistically stable with CNT concentrations from 1 to 15 wt%, probably due to the intrinsic semiconductor behavior of P3HT-CNT composite films in such CNT concentrations (Fig.1b). As a result, the average PCE values of PSCs with CNT concentrations from 1 to 15 wt% in P3HT are similar to those of pristine P3HT-based PSCs. Only for a very high concentration of CNT, 35 wt%, the average J_{SC}, as well as the PCE value, are significantly reduced, probably due to highly concentrated CNT at the perovskite/P3HT-CNT35wt% interface that act as charge recombination centers of the solar cells (Alvarado-Tenorio *et al.*, 2016).

Contrary to CNT, the addition of rGO in P3HT does give a clear tendency of PSCs photovoltaic parameters as a function of rGO concentration in P3HT.

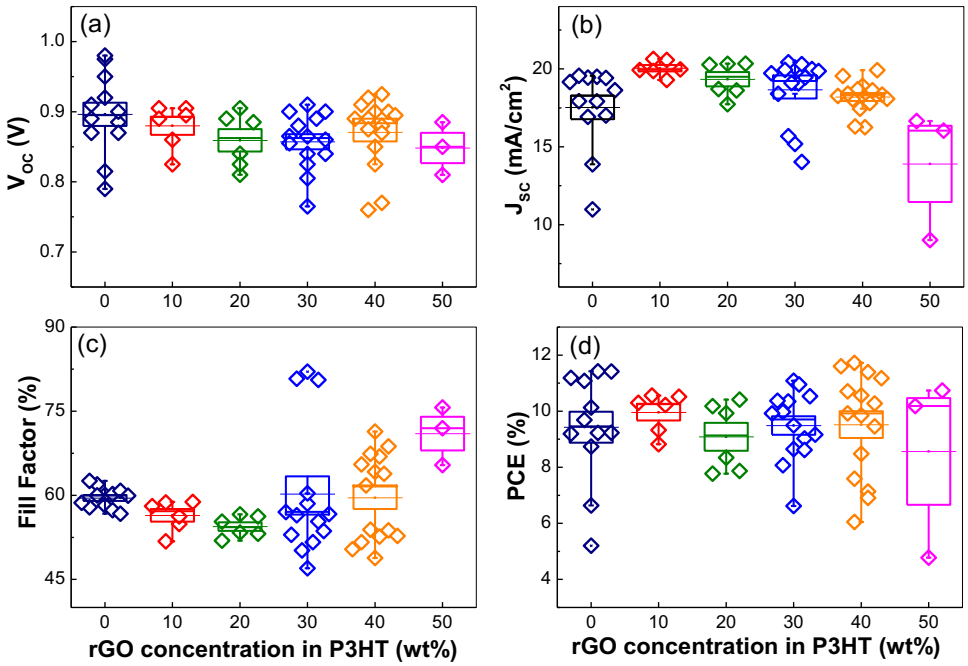

Figure 6. (a) V_{OC}, (b) J_{SC}, (c) FF and (d) PCE of PSCs with P3HT-reduced graphene oxide (rGO) composite films as hole transport layers. The weight percentage of rGO in P3HT varies from 10 to 50%.

Fig.6 indicates that the average V_{OC} values of P3HT-rGO based PSCs gradually decrease with concentration of rGO in P3HT, while the average J_{SC} values increase slightly for rGO concentration up to 30 wt%. It seems that an improved ohmic behavior of the P3HT-rGO composite thin films (Fig.1b) improves at the same time the charge transfer at the P3HT-rGO/Au electrode, leading to higher J_{SC} values of the PSCs. However, the very good distribution of rGO in P3HT matrices also increases the rate of charge carrier recombination at the perovskite/P3HT-rGO interface, reducing slightly the V_{OC} values of PSCs. It is also observed that the FF values of this group of PSCs are in general higher than those of P3HT-CNT PSCs (Fig.5), consequently, both the average and the maximum PCEs of P3HT-rGO-based PSCs are slightly higher than those of pristine P3HT based ones. Finally, as in the case of P3HT-CNT, the very high percentage of rGO in P3HT (50 wt%) markedly reduces the J_{SC} and PCE values of the corresponding PSCs.

To further improve the ohmic contact between P3HT and Au, we took the results of our previous work, which demonstrate that the addition of conductive carbon paint (CP) between the P3HT layer and the Au contact can improve the charge extraction/injection on the Au electrode (Cortina-Marrero *et al.*, 2013). Three types of PSCs have been chosen to test the effect of CP addition: with P3HT (P3HT/CP), P3HT-rGO10 wt% (+rGO10/CP) or P3HT-CNT10 wt% (+CNT10/CP) as HTL. Fig.7 shows that the addition of the CP layer slightly increases the V_{OC} values, except for the P3HT-CNT 10 wt% sample, and, at the same time, decreases the J_{SC} values in all the cases. The most notable change is that the addition of CP significantly increases fill factor (FF), from 7 to 12%, and as a result, PCE values of all PSCs. From these results, we confirm that the P3HT/CP/Au contact is more efficient for charge transfer at the anode of P3HT-based PSCs. The best perovskite solar cell prepared under ambient conditions with P3HT/CP as the hole transport layer gives a V_{OC} of 0.92 V, a J_{SC} of 18.5 mA/cm^2, a FF of 70% and a PCE of 12%.

Finally, the PCE stability of the best P3HT PSCs is measured and shown in Fig.8. Four types of P3HT layers were chosen as HTL in PSCs: pristine P3HT (Fig.8a), P3HT-CNT 10 wt% (Fig.8b), P3HT-rGO 40 wt% (Fig.8c), and P3HT with CP layer (Fig.8d). All cell samples were tested under continuous illumination for approximately 30 min. PSCs with the pristine P3HT are observed to show

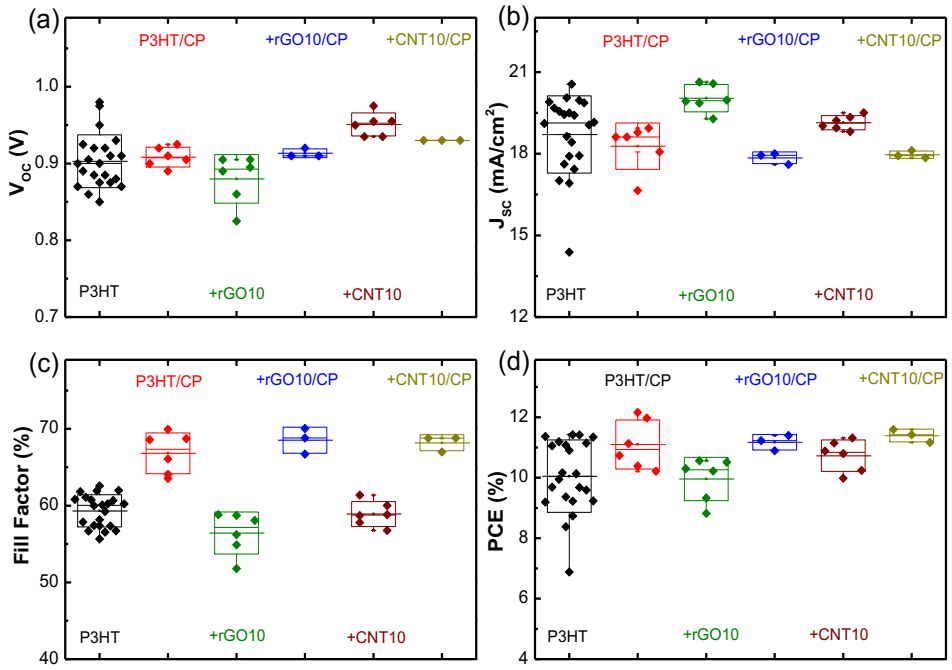

Figure 7. (a) V_{OC}, (b) J_{SC}, (c) FF and (d) PCE of PSCs with different P3HT layers, without and with carbon paint (CP) between P3HT and Au.

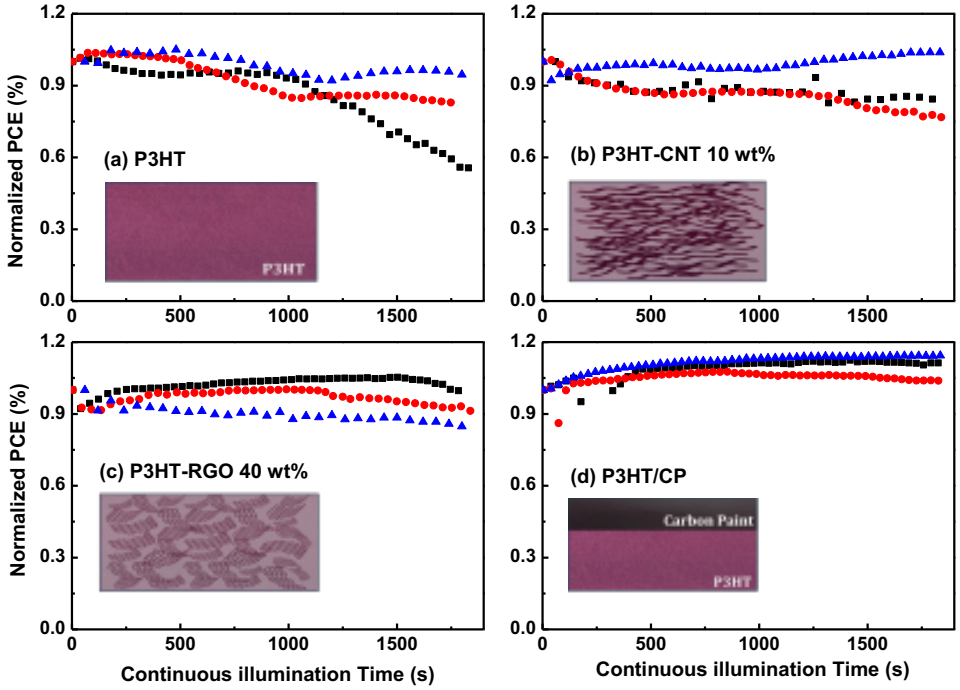

Figure 8. Power conversion efficiencies (PCEs) of PSCs with different hole transport layers: (a) pristine P3HT, (b) P3HT-CNT 10 wt%, (c) P3HT-rGO 40 wt%, and (d) P3HT/CP.

the highest PCE loss, about 25%, after continuous illumination. Those with P3HT-CNT10 wt% lose on average about 13% of PCE. PSCs with P3HT-rGO 40 wt% give better stability, losing on average about 9% of PCE after continuous illumination. The latter two data are better than spiro-OMeTAD-based PSCs that showed a loss of about 20% of their original PCE after the same period of continuous illumination (Torres-Herrera *et al*., 2020). The best stability of PSCs occurs in those PSCs samples that contain a CP layer between the P3HT and Au contact (Fig.8d). No apparent PCE loss is observed after continuous illumination for 30 min, which is the best stability reported for PSCs prepared under similar conditions.

From all the photovoltaic parameters of PSCs with different P3HT composite films, we observe that the addition of CNT or rGO in P3HT leads to a different electrical behavior of P3HT composite films as well as of the corresponding PSCs. This difference should come from different microscopic structures of P3HT-CNT and P3HT-rGO composite thin films. Carbon nanotubes are one-dimensional fibers, and reduced graphene oxides consist of two-dimensional graphene sheets. Since electrical transport in solar cells is in the film thickness direction, the accommodation of carbon products in that direction is very important. With micrometer length, carbon nanotubes should be mainly arranged parallel to the surface of the P3HT composite film, as suggested by their relatively low roughness in AFM images (Fig. 2b and 2c). Since the electric flow has a direction perpendicular to the film surface, the electron conduction should be carried out by hopping between nanotubes. The relatively lower electrical conduction and semiconductor feature of P3HT-CNT composite films confirm the suggested microstructure of P3HT-CNT composite films (Inset of Fig.8b). On the other hand, graphene sheets are relatively short, giving a size of 250 to 550 nm (Becerra-Paniagua *et al*., 2019; Becerra-Paniagua *et al*., 2020). Consequently, they can be randomly distributed within the P3HT matrices, as suggested by the higher surface roughness observed in the P3HT-rGO films (Fig.2e and 2f). This three-dimensional distribution of graphene sheets inside the P3HT-rGO films (inset of Fig.8c) should be the origin of their ohmic conduction over the entire voltage range. Furthermore, the enhancement of the stability of PSCs with the addition of rGO in P3HT should also be related to the microstructure of P3HT-rGO composite films. Light is incident from the FTO glass substrate side of the perovskite solar cell (see Scheme 1a), and not from the HTL (P3HT). The remarkably high optical absorbance spectrum of the P3HT-rGO sample (Fig.1a) suggests that such material should be more compact than P3HT or P3HT-CNT films. Therefore, if P3HT-rGO layer is highly compact, the oxygen or moisture molecules would penetrate less into the perovskite/P3HT-rGO interface and the efficiency of the solar cell would survive more. Three-dimensionally distributed rGO sheets within P3HT seem more effective than two-dimensionally aligned CNT in forming more compact P3HT composite films and reducing O_2/H_2O penetration at the perovskite/HTL interface under continuous illumination test conditions. Finally, a conductive carbon paint sprayed over any P3HT film would reduce the porosity of the HTL film and creates a better mechanical barrier to protect PSCs.

It is important to mention that the efficiencies of PSCs reported in this work are considerably lower than those reported elsewhere (Nia *et al*., 2017; Nia *et al*., 2018, Nia *et al*., 2021, Nia *et al*., 2019; Wu *et al*., 2022). The reasons could be: (1) the lower molecular weight (MW) of our P3HT products (28 kDa), (2) the simple perovskite compound used in this work (MAPbI3-xClx), and (3) no interfacial modification during our PSC preparation. PSC efficiencies of 16-19% reported in Nia *et al*., (2017, 2018, 2019, 2021) were obtained with P3HT with higher MW (100-300 kDa) and hygroscopic lithium salt as doping agents. Another factor that could influence on the efficiencies of PSCs is the thickness of mesoporous TiO_2 (m-TiO_2) layers. As mentioned in Nia *et al*., (2017), PSCs based on 500 nm thick m-TiO_2 reported higher efficiencies than those with 250 nm thick m-TiO_2. In our PSCs, the thickness of the m-TiO_2 layers was about 220 nm, however, the average efficiencies of our pristine P3HT-based PSCs, 9.40%, are much higher than those reported in Nia *et al*., (2017) with a similar thickness of m-TiO_2 (250 nm) and MW of P3HT (44 kDa), 4.92%. On the other hand, in the case of Wu *et al*., (2022), the FAI treatment on the $MAPbI_{3-x}Cl_x$ surface helps to improve the efficiencies of the PSCs. Although the results of those papers suggest that the low efficiencies of our PSCs could be significantly improved if higher MW of P3HT and modified perovskite were used, none of those papers have reported on the stability of non-encapsulated cells under continuous illumination. Our previous works demonstrated that an 80% retain of the original PCE values after 27 min of continuous illumination equals to an 80% retain after 6 months of air storage (Arias-Ramos *et al*., 2020; Torres-Herrera *et al*., 2020). This indicates that our PSCs with carbon paint would keep

100% of their original efficiencies after 6 months of storage in air, much more stable than highly efficient PSCs reported elsewhere.

Conclusions

The modifications of low molecular weight pristine poly(3-hexylthiophene) (P3HT) by $FeCl_3$ doping or addition of carbon nanotubes (CNT) or reduced graphene oxide (rGO) impact in different ways on the electrical behavior and surface morphology of resulting P3HT films. The $FeCl_3$-doped P3HT and P3HT-rGO films show an ohmic behavior, while the P3HT-CNT composites keep a semiconductor characteristic like the pristine P3HT. The ohmic and compact P3HT-rGO composite films give the best power conversion efficiency (PCE) and stability of perovskite solar cells (PSCs) compared to other P3HT materials studied in this work. The addition of conductive carbon paint (CP) between P3HT and the gold contact improves the PCE and stability of PSCs as well, regardless of the type of P3HT films. Without interfacial modification in $MAPbI_{3-x}Cl_x$ or hygroscopic additive in P3HT, the best perovskite solar cell prepared under ambient conditions with P3HT/CP as hole transport layer gives a V_{OC} of 0.92 V, J_{SC} of 18.5 mA/cm^2, FF of 70% and a PCE of 12%, which remains unchanged after a continuous illumination for 30 min. It is concluded that modifications of P3HT-based anodes with carbon materials enhance both the efficiency and stability of PSCs.

Acknowledgments

The authors thank Maria Luisa Ramón-García for XRD measurement and Gildardo Casarrubias-Segura for technical support in solar simulator and AFM. CFAR, JCC, DKBP, WEGP and MAMF acknowledge Consejo Nacional de Ciencia y Tecnología (CONACyT-México) for PhD and FHG, for posdoctorate scholaships. Financial supports from DGAPA -PAPIIT- UNAM (IN104422) and CONACyT Labratorio Nacional LIFyCS (315801) are acknowledged.

References

Alvarado-Tenorio, G., Cortina-Marrero, H.J., Nicho, M.E., Márquez Aguilar, P.A., Hu, H. (2016). Improvement of photovoltaic performance of inverted hybrid solar cells by adding single-wall carbon nano tubes in poly (3-hexylthiophene). *Materials Science in Semiconductor Processing 56*, 37- 42. doi: 10.1016/j.mssp.2016.07.018

Arenas, M.C., Mendoza, N., Cortina, H., Nicho, M.E., Hu, H. (2010). Influence of poly(3-octylthiophene) (P3OT) film thickness and preparation method on photovoltaic performance of hybrid ITO/CdS/P3OT/Au solar cells. *Solar Energy Materials & Solar Cells 94*, 29-33. doi: 10.1016/j.solmat.2009.04.013

Arias-Ramos, C. F., Kumar, Y., Abrego-Martínez, P.G., Hu, H. (2020). Efficient and stable hybrid perovskite prepared at 60% relative humidity with a hydrophobic additive in anti-solvent. *Solar Energy Materials & Solar Cells 215*, 110625. doi: 10.1016/j.solmat.2020.110625

Becerra-Paniagua, D. K., Sotelo-Lerma, M., Hu, H. (2019). Highly oxidized and exfoliated graphene using a modified Tour approach. *Journal of Materials Science: Materials in Electronics 30*, 3973-3983. doi: 10.1007/s10854-019-00683-9

Becerra-Paniagua, D. K., Cabrera-German, D., Díaz-Cruz, E.B., Montiel-González, Z., Sotelo-Lerma, M., Hu, H. (2020). Dispersion degree and sheet spacing control of graphene products via oxygen functionalities and its effect on electrical conductivities of P3HT-graphene composite coatings. *Journal of Materials Science: Materials in Electronics 31*, 19623-19637. doi: 10.1007/s10854-020-04489-y

Chu, Q.-Q., Ding, B., Peng, J., Shen, H., Li, X., Liu, Y., Li, C.-X., Li, C.-J., Yang, G.-J., White, T. P., Catchpole, K. R. (2019). Highly stable carbon-based perovskite solar cell with a record efficiency of over 18% via hole transport engineering. *Journal of Materials Science & Technology 35*, 987-993. doi: 10.1016/j.jmst.2018.12.025

Frost, J.M., Butler, K.T., Brivio, F., Hendon, C.H., Schilfgaarde, M.v., Walsh, A. (2014). Atomistic Origins of High-Performance in Hybrid Halide Perovskite Solar Cells. *Nano Letters 14*, 2584-2590. doi: 10.1021/nl500390f

Ghoreishi, F. S., Ahmadi, V., Alidaei, M., Roghabadi, F. A., Samadpour, M., Poursalehi, R., Johansson, E. M. J. (2022). Enhancing the efficiency and stability of perovskite solar cells based on moisture-resistant dopant free hole transport materials by using a 2D-BA2PbI4 interfacial layer. *Physical Chemistry & Chemical Physics 24*, 1675 - 1684. doi: 10.1039/d1cp04863e

Cortina-Marrero, H. J., Nair, P.K., Hu, H. (2013). Conductive carbon paint as an anode buffer layer in inverted CdS/Poly(3-hexylthiophene) solar cells. *Solar Energy 98*, 196-202. doi: 10.1016/j.solener.2013.09.034

Green, M, Dunlop, E., Hohl-Ebinger, J., Yoshita, M., Kopidakis, N., Hao, X. (2021). Solar cell efficiency tables (Version 57). *Progress in Photovoltaic: Research and Applications 29*, 3-15. doi: 10.1002/pip.3371

Gu, W.-M., Jiang, K.-J., Li, F., Yu, G.-H. , Xu, Y., Fan, X.-H., Gao, C.-Y., Yang, L.-M., Song, Y. (2022). A multifunctional interlayer for highly stable and efficient perovskite solar cells based on pristine poly(3- hexylthiophene). *Chemical Engineering Journal 444*, 136644. doi: 10.1016/j.cej.2022.136644

Guo, Z., Jena, A. K., Takei, I., Ikegami, M., Ishii, A., Numata, Y., Shibayama, N., Miyasaka, T. (2021). Dopant-Free Polymer HTM-Based $CsPbI_2Br$ Solar Cells with Efficiency Over 17% in Sunlight and 34% in Indoor Light. *Advanced Functional Materials 31*, 2103614. doi: 10.1002/adfm.202103614

Habisreutinger, S. N., Leijtens, T., Eperon, G. E., Stranks, S. D., Nicholas, R. J., Snaith, H. J. (2014). Carbon nanotube/polymer composites as a highly stable hole collection layer in perovskite solar cells. *Nano Letters 14*, 5561-5568. doi: 10.1021/nl501982b

Hernández-Guzmán, F., Nicho-Díaz, M.E., Medrano-Solís, A., Altuzar-Coello, P. (2017). In-situ synthesis by Grignard Metathesis of poly(3-hexylthiophene) in presence of CdS and their properties. *European Polymer Journal 90*, 407-417. Doi: 10.1016/j.eurpolymj.2017.03.040

Jeong, M. J., Yeom, K. M., Kim, S. J., Jung, E. H., Noh, J. H. (2021). Spontaneous interface engineering for dopant-free poly(3-hexylthiophene) perovskite solar cells with efficiency over 24%. *Energy & Environmental Science 14*, 2419-2428. doi: 10.1039/d0ee03312j

Joshi, P.H., Zhang, L., Hossain, I.M., Abbas, H.A., Kottokkaran, R., Nehra, S.P., Dhaka, M., Noack, M., Dalal, V.L. (2016). The physics of photon induced degradation of perovskite solar cells. *AIP Advances 6*, 115114, doi: 10.1063/1.4967817

Jung, E. H., Jeon, N. J., Park, E. Y., Moon, C. S., Shin, T. J., Yang, T.-Y., Noh, J. H., Seo, J. (2019). Efficient, stable and scalable perovskite solar cells using poly(3-hexylthiophene). *Nature 567*, 511- 515. doi: 10.1038/s41586-019-1036-3

Kassem, H., Salehi, A., Kahrizi, M., Mirzanejad, H., Hedayati, A., Khorasani, B. (2022). Poly(N,N0-bis-4-butylphenyl-N,N0-biphenyl)benzidine as interfacial passivator for dopant-free P3HT hole transport layer-based perovskite solar cell in regular mesoscopic architecture. *Energy Technologies 10*, 2100956. doi: 10.1002/ente.202100956

Kim, H.-S., Seo, J.-Y, Park, N.-G. (2016). Material and device stability in perovskite solar cells. *ChemSusChem 9*, 2528 - 2540. doi: 10.1002/cssc.201600915

Kim, H.-S., Yang, B., Stylianakis, M. M., Kymakis, E., Zakeeruddin, S. M., Grätzel, M., Hagfeldt, A. (2020). Reduced graphene oxide improves moisture and thermal stability of perovskite solar cells. *Cell Reports Physical Science 1*, 100053. doi: 10.1016/j.xcrp.2020.100053

Krishna, B.G, Ghosh, D.S., Tiwari, S. (2021). Progress in ambient air-processed perovskite solar cells: Insights into processing techniques and stability assessment. *Solar Energy 224*, 1369-1395, doi: 10.1016/j.solener.2021.07.002

Kwan, C.-P., Street, M., Mahmood, A., Echtenkamp, W., Randle, M., He, K., Nathawat, J., Arabchigavkani, N., Barut, B., Yin, S., Dixit R., Singisetti, U., Binek, C., Bird, J.P. (2019). Space-charge limited conduction in epitaxial chromia films grown on elemental and oxide-based metallic substrates. *AIP Advances 9*, 055018. doi: 10.1063/1.5087832.

Li, N., Feng, A., Guo, X., Wu, J., Xie, S., Lin, Q., Jiang, X., Liu, Y., Chen, Z., Tao, X. (2022). Engineering the hole extraction interface enables single-crystal MAPbI3 perovskite solar cells with efficiency exceeding 22% and superior indoor response. *Advanced Energy Materials 12*, 2103241. doi: 10.1002/aenm.202103241

Loewe, R.S., Khersonsky, S.M., McCullough, R.D. (1999). A simple method to prepare head-to-tail coupled, regioregular poly(3-alkylthiophenes) using Grignard Metathesis. *Advanced Materials 11*, 250-253. doi: 10.1002/(SICI)1521-4095(199903)11:3<250::AID-ADMA250>3.0.CO;2-J

Nia, N. Y., Matteocci, F., Cina, L., Di Carlo, A. (2017). High-efficiency perovskite solar cell based on poly(3-hexylthiophene): Influence of molecular weight and mesoscopic scaffold layer. *ChemSusChem 10*, 3854 - 3860. doi: 10.1002/cssc.201700635

Nia, N. Y., Zendehdel, M., Cina, L., Matteoccia, F., Di Carlo, A. (2018). A crystal engineering approach for scalable perovskite solar cells and module fabrication: a full out of glove box procedure. *Journal of Materials Chemistry A6*, 659-671. doi: 10.1039/c7ta08038g

Nia, N. Y., Lamanna, E., Zendehdel, M., Palma, A.L., Zurlo, F., Castriotta, L.A., Di Carlo, A. (2019). Doping strategy for efficient and stable triple cation hybrid perovskite solar cells and module based on poly(3-hexylthiophene) hole transport layer. *Small 15*, 1904399. doi: 10.1002/smll.201904399.

Nia, N. Y., Bonomo, M., Zendehdel, M., Lamanna, E., Desoky, M.M.H., Paci, B., Zurlo, F., Generosi, A., Barolo, C., Viscardi, G., Quagliotto, P., Di Carlo, A. (2021). Impact of P3HT regioregularity and molecular weight on the efficiency and stability of perovskite solar cells. *ACS Sustainable Chemical Engineering 9*, 5061-5073. doi: 10.1021/acssuschemeng.0c09015

Ono, L. K., Schulz, P., Endres, J. J., Nikiforov, G. O., Kato, Y., Kahn, A., Qi, Y. (2014). Air-exposure-induced gas-molecule incorporation into spiro-MeOTAD films. *Journal of Physical Chemistry Letters 5*, 1374-1379. doi: 10.1021/jz500414m

Peng, J., Kremer, F., Walter, D., Wu, Y., Ji, Y., Xiang, J., Liu, W., Duong, T., Shen, H., Lu, T., Brink, F., Zhong, D., Li,L., Lee, O., Lem, C., Liu, Y., Weber, K.J., White, T.P., Catchpole, K.R. (2022). Centimetre-scale perovskite solar cells with fill factors of more than 86 per cent. *Nature 601*, 573-578. doi: 10.1038/s41586-021-04216-5

Schulz, P., Edri, E., Kirmayer, S., Hodes, G., Cahen, D., Kahn, A. (2014). Interface energetics in organo-metal halide perovskite-based photovoltaic cells. *Energy & Environmental Science 7*, 1377-1381. doi: 10.1039/c4ee00168k

Sharma, R., Sharma, A., Agarwal, S., Dhaka, M.S. (2022). Stability and efficiency issues, solutions and advancements in perovskite solar cells: A review. *Solar Energy 244*, 516-535. doi: 10.1016/j.solener.2022.08.001

Snaith, H.J., Grätzel, M. (2007). Light-Enhanced Charge Mobility in a Molecular Hole Transporter. *Physical Review Letters 98*, 177402. doi: 10.1103/PhysRevLett.98.177402

Torres-Herrera, D. M., Moreno-Romero, P. M. Cabrera-German, D., Cortina-Marrero, H. J. Sotelo-Lerma, M., Hu, H. (2020). Thermal co-evaporated MoOx:Au thin films and its application as anode modifier in perovskite solar cells. *Solar Energy 206*, 136-144. doi: 10.1016/j.solener.2020.05.105

Younas, M., Kandiel, T.K., Rinaldi, A., Peng, Q., Al-Saadi, A.A. (2021). Ambient-environment processed perovskite solar cells: A review. *Materials Today Physics 21*, 100557, doi: 10.1016/j.mtphys.2021.100557

Wu, G., Dong, X., Cui, G., Sun, R., Wu, X., Gu, M., Zuo, Z., Liu, Y. (2022). A facile strategy for

high performance air-processed perovskite solar cells with dopant-free poly(3-hexylthiophene) hole transporter. *Solar Energy 237*, 153- 160. doi: 10.1016/j.solener.2022.03.063

Zhang, W., Wan, L., Fu, S., Li, X., Fang, J. (2020). Reducing energy loss and stabilising the perovskite/poly (3-hexylthiophene) interface through a polyelectrolyte interlayer. *Journal of Materials Chemistry A 8*, 6546-6554. doi: 10.1039/d0ta01860k